08.1

System approach to the analysis of solar cell efficiency: mesostructured perovskite solar cell

© *F. Bonnin-Ripoll*[1], *R. Pujol-Nadal*[1], *Y.B. Martynov*[2], *V.A. Kinev*[3], *R.G. Nazmitdinov*[3,4]

[1] Faculty of Industrial Engineering and Construction, University of the Balearic Islands, Palma, Spain
[2] Scientific and Production Enterprise „Istok" named after Shokin, Fryazino, Moscow Region, Russia
[3] State University „Dubna", Dubna, Moscow Region, Russia
[4] The N.N. Bogolyubov Laboratory of Theoretical Physics, Joint Institute for Nuclear Research, Dubna, Moscow Region, Russia
E-mail: rashid@theor.jinr.ru

Received October 5, 2023
Revised November 9, 2023
Accepted November 9, 2023

A method for analyzing the photocell efficiency is proposed, based on the procedure of statistical averaging of experimental data. The method enables an assessment of the overall quality of the device and to determine the conditions for increasing its efficiency by optimizing the functional layers thicknesses. By means of the developed approach, the characteristics of the functional layers of the experimental perovskite solar cell with a mesoporous TiO_2 layer were established, and the excellent agreement between the theoretical and experimental values of the current-voltage characteristics was obtained.

Keywords: perovskite solar cell, thin film, mesoporous, optoelectronic measurements and analysis, energy conversion efficiency.

DOI: 10.61011/TPL.2024.02.57983.19752

Due to their remarkable electrical and optical properties, organic-inorganic halide perovskites (OIHPs) attract great attention of researchers due to their potential for using as light-absorbing material in the field of photovoltaics. Photovoltaic cells with OIHP-layers, for which an energy conversion efficiency of 25.8% [1] has recently been achieved, are the most promising competitors of silicon-based photovoltaic cells. Cheap production, high radiation absorption coefficient, big diffusion length and high mobility of charge carriers, as well as a high power conversion efficiency (PCE) are undoubted advantages of OIHPs. Moreover, various modifications of perovskite compositions are being actively developed today for the purpose of achieving their great stability and utilization in wide ranges of absorbed radiation [2]. Obviously, the analysis of the optical and electrical properties of different functional layers in the device architecture is crucial for further improvement of the efficiency of perovskite solar cells (PSCs). However, some parameters of these layers are hard to measure. For example, estimates of charge carrier's mobility in perovskite are quite approximate. Problems also arise when measuring the thicknesses of different functional layers of an experimental sample of PSC. Thicknesses can vary not only from sample to sample, but also for an individual synthesized layer of the sample. One of the main goals of this work is to elaborate an efficient approach combining the analysis of optical and electrical properties of mesostructured PSC that allow to obtain an objective estimate of the properties of different functional layers of the experimental sample.

To achieve this goal, we will analyze the properties of PSC with a well-proven architecture (Fig. 1), which was fabricated by us using the methodology of the work [3]. The device looks like a $n-i-p$-diode. A thin and compact layer TiO_2 (c-TiO_2) was applied on a complex glass substrate to facilitate the collection of photogenerated electrons from the perovskite material. To improve the efficiency of charge carriers collection, a layer of mesoporous TiO_2 (mp-TiO_2) was introduced to improve the further growth of perovskite. Moreover, partial infiltration of perovskite into the layer of mp-TiO_2 reduces the number of traps at that boundary. To improve the hole transfer between perovskite and gold electrode we used Spiro-OMeTAD ($C_{81}H_{68}N_4O_8$). Note that at the moment there is no consistent methodology for determining the thickness of the mesoporous layer and its quantitative effect on the PCE for PSC. Then, we considered an efficient approach to the analysis of the optical and electric characteristics both of the mp-TiO_2 layer and the device as a whole.

Since electronic and optical measurements cannot be performed on the same PSC sample, two batches of 24 samples made in the same conditions were prepared. The first batch was used for optical measurements with interruptions at each phase of the process of PSC fabrication, and the second — for the measurements of current-voltage curves (CVC).

Considering the application of a new layer of material as a separate stage of the process, we measured the optical transmittance of the obtained structure ($T^{exp}(\lambda)$) for a given interval of wavelengths λ. At the stage 1, a multilayer glass substrate was fabricated, which is formed by the layers of SnO_2, SiO_2 and fluorine-doped tin oxide (FTO). At the stage 2, a layer of c-TiO_2 with a thickness about dozens of nanometers was added by spray pyrolysis. Then,

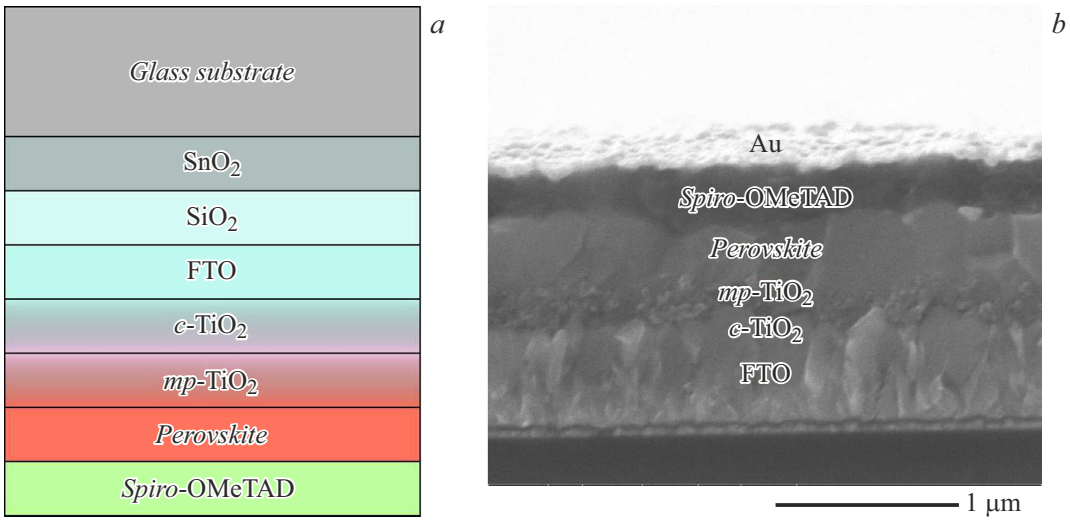

Figure 1. *a* —schematic image of the architecture of the experimental PSC layers; *b* —typical image of the experimental sample obtained by means of scanning electron microscope.

Table 1. The range of thicknesses of the layers of the material in PSC samples measured by scanning electron microscopy

Material	Thickness, nm
SiO_2	10–30
SnO_2	10–30
FTO	500–600
c-TiO_2	10–30
mp-TiO_2	180–300
Perovskite	400–550
Spiro-OMeTAD	200–250

at the stage 3, a layer of *mp*-TiO_2 was deposited, which was followed by application of perovskite (stage 4) and Spiro-OMeTAD (stage 5). The last three layers were applied by centrifugation. Then, we measured CVC of PSC for the second batch of 24 samples by means of a solar energy simulator. These measurements resulted in the mean value of short-circuit current for $J_{sc}^{exp} = 20.07\,\text{mA/cm}^2$ with a standard deviation of $0.99\,\text{mA/cm}^2$ at an illumination of $1000\,\text{W/m}^2$. Measurements of the transmittance of the whole device were performed using a UV-VIS CARY 4000 spectrophotometer at normal incidence within the wavelength range of 200–800 nm. Our measurements showed that it is sufficient to fabricate six samples at each stage to get a reliable result for the mean value. The approximate thickness of each layer of the material (Table 1) was estimated by means of scanning electron microscopy techniques.

To theoretically analyze the amount of transmitted $T^{th}(\lambda)$, absorbed $\alpha(\lambda)$, and reflected light in each of the materials forming the PSC architecture, we used ray tracing simulation by means of the OTSun python software package [4]. The simulation is based on the Monte Carlo method. At that, the optical characteristics were described by using the Fresnel equations in their most general form with the addition of the transfer matrix method (TMM) to consider the interference phenomenon [5] (see details in [6]).

The complex refraction indices of the following materials were taken from the reference publications: FTO [7], TiO_2 [8], Spiro-OMeTAD [9]. In the case of SnO_2 and SiO_2, data from the material manufacturer were used. The refraction index of the glass was calculated based on the transmittance measurements. An average volume theory model was used to determine the complex index of the material *mp*-TiO_2 [10]. Properties of *mp*-TiO_2 were associated with efficient medium containing the mixture of *c*-TiO_2 and air (see below). The complex refraction index of perovskite ($FAPbI_3$) was taken from the work [11].

For comparison of theoretical and experimental transmittance values, it is necessary to determine the combinations of thicknesses of functional layers (hereinafter referred to as configuration) of the PSC structure. Using the measured value ranges (Table 1), we calculated the sample configuration at each stage of the fabrication process using TMM to get the best concordance with the experimental data. In order to achieve our goal, we calculated the root-mean-square error (RMSE)

$$\text{RMSE} = \frac{1}{N}\sqrt{\sum_{\lambda=300}^{\lambda=800}\left[T^{exp}(\lambda) - T^{th}(\lambda)\right]^2}. \qquad (1)$$

Here N —is the total number of steps for a given interval of wavelength with the increment of 1 nm. For example, at first, we performed calculations for the stage 1 considering configurations from the following thickness ranges (nm): 10–30 for SnO_2 and SiO_2, 500–600 for FTO. As a result, we selected configurations that fall within 1% of the least RMSE. Then, similar calculations were performed for

Table 2. Characteristics of the semiconductors in question: TiO_2, $FAPbI_3$ (perovskite), Spiro-OMeTAD (for the model [14])

Parameter	Layers			
	c-TiO_2	mp-TiO_2	Perovskite	Spiro-OMeTAD
χ, eV	4	4	3.75	2.12
E_g, eV	3.05	3.05	1.66	3.1
m_e^*/m_e	1	1	1	1
m_h^*/m_e	1	1	1	1
$N_{d/a}$, cm^{-3}	$1 \cdot 10^{18}$	Variable	0	$1 \cdot 10^{21}$
μ, $cm^2/(V \cdot s)$	0.006	0.006	Variable	0.0001
ε	60	**42.45**	60	3
l_D, nm	4	4	Variable	0.5

Note. χ — electron affinity, E_g — band gap width, $m_{e/h}^*/m_e$ — effective mass of electron/hole, $N_{d/a}$ — concentration of donors/acceptors, μ — mobility, ε — permittivity, l_D — diffusion length. Determination of the permittivity of mp-TiO_2 (the value is highlighted bold) is discussed in the text (see equation (2)).

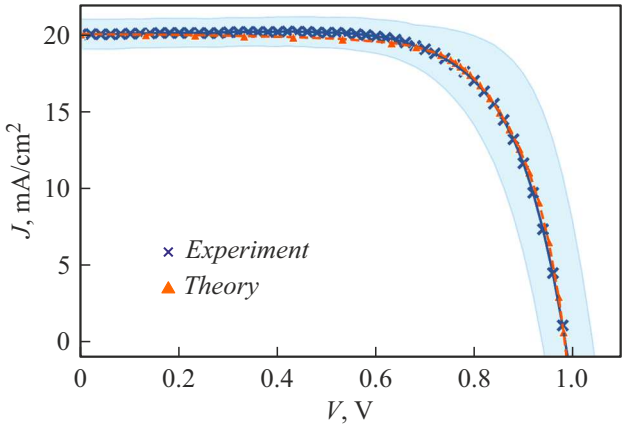

Figure 2. Current-voltage curves. A wide band around the experimental curve indicates the boundaries of deviations from the mean value when measuring experimental samples.

subsequent stages, subject to the reduced ranges found at the previous stage.

The thickness values that gave the best match between the measured short-circuit current J_{sc}^{exp} and the theoretical value J_{sc}^{th} were considered as final mean values of layer thicknesses in the fabricated PSCs. The method proposed in [12] and the TMM library [13] were used for the calculation of J_{sc}^{th}. The results of the short-circuit current calculations showed relatively small sensitivity to the change in thickness of perovskite and Spiro-OMeTAD. According to our analysis, an „optimum“ configuration having the best correlation with the obtained experimental data had the following thicknesses (nm): 11 (SiO_2), 16 (SnO_2), 565 (FTO), 24 (c-TiO_2), 240 (mp-TiO_2, porosity 20%), 500 (perovskite), 250 (Spiro-OMeTAD).

Using the „optimum“ configuration of thicknesses, we calculated the CVC of PSC by solving the transport model equations [14]. The input parameters were the characteristics of the functional layers (Table 2). There were „variable“ parameters in them. Their values were determined based on the condition of the best match of the measured mean and calculated CVC of the PSC.

For example, in order to perform transport model calculations, we had to determine the permittivity and electrical conductivity of the layer of mp-TiO_2 $\sigma_{mp} = q\mu_{mp}N_{mp}$, where μ_{mp} — is the majority charge carriers mobility and N_{mp} — is the dopant concentration. Analysis of the optical properties showed that the mp-TiO_2 layer contains air-filled holes (porosity). Since the concentration of these holes is small (20%), the dielectric permittivity of such a mixture can be approximated by (see details in [15]):

$$\varepsilon_{mix} = \varepsilon_{TiO_2} + c\frac{3(\varepsilon_a - \varepsilon_{TiO_2})\varepsilon_{TiO_2}}{\varepsilon_a + 2\varepsilon_{TiO_2}}, \qquad (2)$$

where ε_{TiO_2} and ε_a — are permittivities of TiO_2 and air, respectively, c — is the air-filled holes concentration. It can be assumed that the electrical conductivity in that layer shall also be reduced by at least 20%. In the calculations, it was assumed that the mobility of carriers remains the same as in the layer of c-TiO_2 ($\mu_{mp} = \mu_c$), while the donors concentration was determined by the ratio of $N_{mp} \leqslant 0.8N_c$, where N_c — is the concentration of donors in the layer of c-TiO_2. Therefore, the following parameters were found based on the condition of the best match between the measured mean and calculated CVC: efficient concentration of donors in the layer of mp-TiO_2 ($N_{mp} = 1 \cdot 10^{17}\,cm^{-3}$), mobility of carriers in the perovskite layer ($\mu = 50\,cm^2/(V \cdot s)$) and the time of their life ($\tau = 0.7\,ns$). This allowed us to estimate the diffusion length in perovskite $l_D = \sqrt{\mu k_B T \tau/|e|} = 0.3\,\mu m$. Note that the values we obtained for N_{mp}/μ fall within the limits known from the referenced publications: $10^{16}-10^{19}\,cm^{-3}$ for N_{mp} [16] and $5-50\,cm^2/(V \cdot s)$ for μ [17]. With these parameters, an excellent correspondence between the calculated and measured averaged CVC was obtained (Fig. 2): short-circuit current $J_{sc}^{exp}(J_{sc}^{th}) = 20.072$ $(20.076)\,mA/cm^2$, open-circuit voltage $V_{oc}^{exp}(V_{oc}^{th}) = 0.985$ $(0.984)\,V$, CVC filling ratio $FF^{exp}/FF^{th} = 0.695(0.703)$, PCE^{exp} $(PCE^{th}) = 13.735(13.882)\%$.

Therefore, the proposed approach allowed us to determine the averaged characteristics of the different functional layers of the experimental sample and its efficiency. This approach can be used to optimize the architecture of the developed PSC for the purpose of obtaining a high PCE of the fabricated sample.

Acknowledgments

F. Bonnin-Ripoll is grateful to the Catalan Institute of Nanoscience and Nanotechnology (ICN2, Barcelona) for the excellent conditions provided to perform the experimental studies.

Funding

This work was financially supported by the Spanish Ministry of Science (project TED2021-132758B-I00, MCIN/AEI/10.13039/501100011033/), the Government of the Balearic Islands (project FPI/2144/2018), and the Russian Science Foundation (project 23-19-00884).

Conflict of interest

The authors declare that they have no conflict of interest.

References

[1] H. Min, D.Y. Lee, J. Kim, G. Kim, K.S. Lee, J. Kim, M.J. Paik, Y.K. Kim, K.S. Kim, M.G. Kim, T.J. Shin, S.I. Seok, Nature, **598**, 444 (2021). DOI: 10.1038/s41586-021-03964-8
[2] X. Yu, H.N. Tsao, Z. Zhang, P. Gao, Adv. Opt. Mater., **8**, 2001095 (2020). DOI: 10.1002/adom.202001095
[3] H. Xie, Z. Wang, Z. Chen, C. Pereyra, M. Pols, K. Gałkowski, M. Anaya, S. Fu, X. Jia, P. Tang, D.J. Kubicki, A. Agarwalla, H.S. Kim, D. Prochowicz, X. Borrisé, M. Bonn, C. Bao, X. Sun, S.M. Zakeeruddin, L. Emsley, J. Arbiol, F. Gao, F. Fu, H.I. Wang, K.J. Tielrooij, S.D. Stranks, S. Tao, M. Grätzel, A. Hagfeldt, M. Lira-Cantú, Joule, **5**, 1246 (2021). DOI: 10.1016/J.JOULE.2021.04.003
[4] G. Cardona, R. Pujol-Nadal, PLoS ONE, **15**, e0240735 (2020). DOI: 10.1371/journal.pone.0240735
[5] S.J. Byrnes, *Multilayer optical calculations* (2020). DOI: 10.48550/arXiv.1603.02720
[6] F. Bonnin-Ripoll, Y.B. Martynov, G. Cardona, R.G. Nazmitdinov, R. Pujol-Nadal, Solar Energy Mater. Solar Cells, **200**, 110050 (2019). DOI: 10.1016/j.solmat.2019.110050
[7] E. Ching-Prado, A. Watson, H. Miranda, Science: Mater. Electron., **29**, 15299 (2018). DOI: 10.1007/s10854-018-8795-8.
[8] T. Siefke, S. Kroker, K. Pfeiffer, O. Puffky, K. Dietrich, D. Franta, I. Ohlídal, A. Szeghalmi, E.-B. Kley, A. Tünnermann, Adv. Opt. Mater., **4**, 1780 (2016). DOI: 10.1002/adom.201600250.
[9] C.W. Chen, S.Y. Hsiao, C.Y. Chen, H.W. Kang, Z.Y. Huang, H.W. Lin, J. Mater. Chem. A, **3**, 9152 (2015). DOI: 10.1039/C4TA05237D
[10] N.J. Hutchinson, T. Coquil, A. Navid, L. Pilon, Thin Solid Films, **518**, 2141 (2010). DOI: 10.1016/J.TSF.2009.08.048
[11] H.W. Chen, D.P. Gulo, Y.C. Chao, H.L. Liu, Sci. Rep., **9**, 18253 (2019). DOI: 10.1038/s41598-019-54636-7
[12] J.M. Ball, S.D. Stranks, M.T. Hörantner, S. Hüttner, W. Zhang, E.J.W. Crossland, I. Ramirez, M. Riede, M.B. Johnston, R.H. Friend, H.J. Snaith, Energy Environ. Sci., **8**, 602 (2015). DOI: 10.1039/C4EE03224A.
[13] S. Byrnes, *tmm 0.1.7: Python Package Index* (2017).
[14] F. Bonnín-Ripoll, Y.B. Martynov, R.G. Nazmitdinov, G. Cardona, R. Pujol-Nadal, Phys. Chem. Chem. Phys., **23**, 26250 (2021). DOI: 10.1039/d1cp03313a
[15] L.D. Landau, E.M. Lifshits. *Elektrodinamika sploshnykh sred* (Nauka, M., 1982) (in Russian), pp. 67–69.
[16] M.C. Sellers, E.G. Seebauer, Thin Solid Films, **519**, 2103 (2011). DOI: 10.1016/J.TSF.2010.10.071
[17] L.M. Herz, ACS Energy Lett., **2**, 1539 (2017). DOI: 10.1021/acsenergylett.7b00276.

Translated by EgoTranslating